

Abstract

Mg / Ca ratios in foraminiferal tests are routinely used as paleo temperature proxy, but on long timescales, also hold the potential to reconstruct past seawater Mg / Ca. Impact of both temperature and seawater Mg / Ca on Mg incorporation in foraminifera have been quantified by a number of studies. The underlying mechanism responsible for Mg incorporation in foraminiferal calcite and its sensitivity to environmental conditions, however, is not fully identified. A recently published biomineralization model (Nehrke et al., 2013) proposes a combination of transmembrane transport and seawater leakage or vacuolization to link calcite Mg / Ca to seawater Mg / Ca and explains inter-species variability in Mg / Ca ratios. To test the assumptions of this model, we conducted a culture study in which seawater Mg / Ca was manipulated by varying $[Ca^{2+}]$ and keeping $[Mg^{2+}]$ constant. Foraminiferal growth rates, test thickness and calcite Mg / Ca of newly formed chambers were analyzed. Results showed optimum growth rates and test thickness at Mg / Ca closest to that of ambient seawater. Calcite Mg / Ca is positively correlated to seawater Mg / Ca, indicating that not absolute seawater $[Ca^{2+}]$ and $[Mg^{2+}]$, but the relative ratio controls Mg / Ca in tests. These results demonstrate that the calcification process cannot be based only on seawater vacuolization, supporting the mixing model proposed by Nehrke et al. (2013). Here we, however, suggest a transmembrane transport fractionation that is not as strong as suggested by Nehrke et al. (2013).

1 Introduction

Foraminiferal test Mg/Ca_{CC} is a proxy used in paleoceanography to reconstruct past seawater temperatures (e.g. Nürnberg et al., 1996; Lear et al., 2000). In addition to temperature, calcite Mg/Ca_{CC} is also controlled by seawater Mg/Ca_{SW} (Segev and Erez, 2006; Evans and Müller, 2012). Since Mg/Ca_{SW} varied over geological time due to changes in the balance between Mg and Ca input and output, paleoceanog-

Impact of seawater Ca^{2+} on the calcification

A. Mewes et al.

Title Page

Abstract

Introduction

Conclusions

References

Tables

Figures



Back

Close

Full Screen / Esc

Printer-friendly Version

Interactive Discussion



Impact of seawater Ca^{2+} on the calcification

A. Mewes et al.

Title Page

Abstract

Introduction

Conclusions

References

Tables

Figures



Back

Close

Full Screen / Esc

Printer-friendly Version

Interactive Discussion



raphers need to account for this ratio in seawater, when using foraminiferal $\text{Mg}/\text{Ca}_{\text{CC}}$ to reconstruct temperatures on timescales beyond ~ 1 Ma. Due to the long residence times of Mg^{2+} (~ 13 Ma) and Ca^{2+} (~ 1 Ma), this ratio does not need to be corrected for when using foraminiferal Mg/Ca on shorter timescales (Broecker and Yu, 2011; Hardie, 1996).

Biological processes involved in calcification complicate the relationships between $\text{Mg}/\text{Ca}_{\text{CC}}$, temperature and $\text{Mg}/\text{Ca}_{\text{SW}}$, which is apparent from large inter-species differences in Mg/Ca (Bentov and Erez, 2006). To improve the reliability of proxy relationships it is hence necessary to understand the impact of cellular processes involved in calcification. Controlled culture studies allow disentanglement of impacts that often co-vary in the field, as well as allowing exceeding naturally existing ranges in conditions. Studies by e.g. Erez (2003), and Bentov et al. (2009) suggested that foraminifers vacuolize seawater to acquire the ions needed for calcification. Seawater vacuolization would require the extraction of Ca^{2+} and CO_3^{2-} from the vacuoles or the removal of all unwanted ions, such as e.g. Mg^{2+} . However, studies by De Nooijer et al. (2009) and Nehrke et al. (2013) showed that the volume of vacuoles observed during calcification cannot account for the total amount of ions needed for calcification. An intracellular storage reservoir for inorganic carbon, or a “pool”, was shown for the perforate foraminifer, *Amphistegina lobifera* (Ter Kuile et al., 1989), possibly corresponding to the vacuoles described by Erez (2003) (De Nooijer et al., 2014). However, Ca^{2+} pools are absent in the benthic *Ammonia aomoriensis*, demonstrated by Nehrke et al. (2013). On the basis of their experiments these authors suggested that selective transmembrane transport (TMT) is responsible for the delivery of Ca^{2+} to the site of calcification during chamber formation. A minor portion of unfractionated elements may reach the site of calcification passively via seawater leakage or via seawater vacuolization (Nehrke et al., 2013). This model predicts a linear relationship between $\text{Mg}/\text{Ca}_{\text{SW}}$ and $\text{Mg}/\text{Ca}_{\text{CC}}$, as observed for e.g. *Amphistegina lessonii* (Segev and Erez, 2006; Mewes et al., 2014), *Amphistegina lobifera* (Segev and Erez, 2006) and *Ammonia aomoriensis* (Mewes et al., 2014). In the experiments by Mewes et al. (2014), $[\text{Ca}]$ was kept constant while $[\text{Mg}]$ was varied.

final culture media were verified by inductively coupled plasma – optical emission spectrometry (ICP-OES) and are summarized in Table 1. Since salinity varied, depending on the varying [Ca], salinity was measured for all treatments (salinometer: WTW, Cond 330) and adjusted to a constant value ($S = 32.4$), by adding NaCl from a stock solution (5 M). pH was measured using a pH meter (WTW, pH 3110, NBS scale) and adjusted to a constant value (pH = 8.01) by adding 1 M NaOH. Total alkalinity (TA) and dissolved inorganic carbon (DIC) were determined using a SI-Analytics TW alpha plus and a XY-2 Sampler, Bran und Luebbe, respectively. All values are summarized in Table 1.

2.3 Juvenile *Amphistegina lessonii*

For the culture experiment, juvenile specimens of *A. lessonii* were used to ensure that most of their calcite is formed during incubation in controlled conditions. To obtain juveniles, adult specimens were picked from the stock material. Adult specimens crawled up the aquarium glass walls, facilitating selection of living specimens, and transferred to well plates. Well plates were placed in light (12 h light/12 h dark cycle) and temperature controlled incubators (RUMED, Rubarth Apparate GmbH) at 25 °C. The daylight sources had a light intensity of $130 \mu\text{mol m}^{-2} \text{s}^{-1}$ at the level of the well plates. After a few days, about 10% of the specimens had reproduced asexually. These juveniles were selected for the culturing experiments and evenly distributed between the different treatments.

2.4 Culture experiment

The culture protocol was the same as reported in Mewes et al. (2014), except for the manipulation of the culture media (compare 2.2). Juveniles of *A. lessonii* were incubated in petri dishes, containing ~ 10 mL of culturing medium. In total, juveniles of 4 different broods were used and divided equally over the treatments (each brood in duplicates containing 5–10 individuals per petri dish), resulting in 50 to 56 juveniles for every treatment. To maintain constant culture conditions, the culture media was replaced

BGD

11, 17463–17489, 2014

Impact of seawater Ca^{2+} on the calcification

A. Mewes et al.

Title Page

Abstract

Introduction

Conclusions

References

Tables

Figures



Back

Close

Full Screen / Esc

Printer-friendly Version

Interactive Discussion



was weighed as a whole, resulting in $n = 8$ (duplicates \times 4 broods) measurements. Mean weight per specimen was determined by dividing the weight of each replicate by the number of specimens in the group. Weight was normalized to the final size measured with the microscope. This size normalized weight (SNW) is an indication for test wall thickness and defined by:

$$\text{SNW} = \frac{\text{weight } [\mu\text{m}]}{\text{size } [\mu\text{m}]} \quad (1)$$

Size normalized weight also depends on the time spend in culture, which makes it challenging to compare SNW measured in our experiment to other experiments. Thus, we expressed size normalized weight as relative SNW [%], such that it is related to the highest SNW in each of the experiments (which equals 100 %).

2.8 Element measurements

Elemental concentrations were determined using laser-ablation inductively coupled plasma mass spectrometry (LA-ICP-MS). For this purpose, analyses were done on the GeoLas 22Q Excimer laser (Lambda Physik), coupled to a sector field ICP-MS (Element 2, Thermo Scientific) at Utrecht University (Reichart et al., 2003). Prior to analyses, specimens were mounted on stubs with double-sided adhesive tape. Depending on the size of the chambers, laser spot size was set to 80, 60 or 40 μm to ablate as much material as possible while at the same time avoiding contamination from adjacent chambers. From each replicate group in each of the treatments, 4–6 chambers of one to two specimens were analyzed, resulting in 50 to 65 measurements per treatment. Data from single chamber measurements were calibrated against a glass standard (SRM NIST 610; Jochum et al., 2011). To assure high signal quality (e.g. to correct for drift), every 10–15 measurements two NIST standards were measured. Laser repetition rate was set to 7 Hz and the energy density was set to $\sim 1.2 \text{ J cm}^{-2}$ when ablating calcite and to $\sim 5 \text{ J cm}^{-2}$ when ablating glas. Elemental concentrations

Impact of seawater Ca^{2+} on the calcification

A. Mewes et al.

Title Page

Abstract

Introduction

Conclusions

References

Tables

Figures



Back

Close

Full Screen / Esc

Printer-friendly Version

Interactive Discussion



This is necessary due to the saturation of growth in the present study after 30 days (Fig. 1a).

Mewes et al. (2014) varied seawater [Mg] and kept [Ca] constant at 10 mM, observing a similar optimum at ambient Mg/Ca_{SW}. An increase of seawater [Mg] from ~ 50 to ~ 90 mM decreased growth rates even more than lowering of [Mg] from ~ 50 to ~ 14 mM. Considering both data sets suggest that the Mg/Ca_{SW} ratio and not the absolute concentrations of Ca or Mg are primarily controlling growth rates. Apparently, the optimum Mg/Ca_{SW} for foraminiferal growth is between 3 and 5 mol mol⁻¹ (Fig. 4). In a similar study, Segev and Erez (2006) measured growth rates in *Amphistegina* spp. as a function of seawater Mg / Ca in terms of CaCO₃ addition, similarly concluding that the Mg / Ca ratio of seawater is the main driver of the specimens' growth rates. Their data suggest that highest growth rate is reached at Mg/Ca_{SW} of ~ 1, while a ratio of ~ 0.5 was suboptimal. Because Mg is known to inhibit inorganic calcite precipitation, they concluded that *Amphistegina* spp. is able to precipitate its test more easily from seawater with lower Mg / Ca ratios. While this argument is based on a comparison with the inorganic system, their explanation for the decline in growth rate at Mg/Ca_{SW} ~ 0.5 mol mol⁻¹ is based on physiology, i.e. that a minimum of Mg is required for foraminiferal growth. This physiological explanation can in itself not fully explain our results, because the lowest Mg/Ca_{SW} in our studies (the present one and Mewes et al., 2014) was achieved through both elevating seawater [Ca] and lowering [Mg]. Interestingly, at low Mg/Ca_{SW}, elevated seawater [Ca] affected growth rate more profoundly than lowered [Mg] (Fig. 4). The latter observation can neither be explained in terms of inorganic calcite precipitation nor in terms of a minimum Mg requirement. However, it may be that high seawater [Ca] may be toxic for the cell (e.g. Martinez-Colon et al., 2009). Together, the results of Segev and Erez (2006) and those presented here strongly suggest that growth in *Amphistegina* spp. is influenced by the Mg/Ca_{SW} ratio with an optimum close to the ratio of natural seawater.

The same argumentation also applies to SNW (Fig. 5). This is the first study showing the effect of Mg/Ca_{SW} on foraminiferal SNW, which is correlated to the change

BGD

11, 17463–17489, 2014

Impact of seawater Ca²⁺ on the calcification

A. Mewes et al.

Title Page

Abstract

Introduction

Conclusions

References

Tables

Figures

◀

▶

◀

▶

Back

Close

Full Screen / Esc

Printer-friendly Version

Interactive Discussion



in growth rates as a function of Mg/Ca_{sw} . Similar trends for growth rate and SNW in response to seawater carbonate chemistry changes were described for another benthic foraminifer, namely *Ammonia tepida* (i.e. *A. aomoriensis*) (Keul et al., 2013). It should be emphasized that comparison of absolute values for SNW or growth rate between different experiments is challenging since observed values are highly variable, even under similar culture conditions. This phenomenon is not confined to foraminifers, but also known from culture studies using coccolithophores (Hoppe et al., 2011). It is therefore reasonable to follow the recommendation of Hoppe et al. (2011) and base interpretations on response patterns, i.e. trends, rather than absolute values.

4.2 Calcite Mg / Ca

Our results show that Mg/Ca_{CC} increases linearly with decreasing seawater $[Ca]$ and thus increasing Mg/Ca_{sw} (Fig. 3a). Comparison to our previous study, where $[Mg]$ was varied and $[Ca]$ was kept constant (Mewes et al., 2014) shows a strong agreement between the two data sets (Fig. 6a). This suggests that test Mg/Ca_{CC} is controlled by the ratio of Mg to Ca in seawater, rather than by absolute concentrations. This result could be in accordance with a calcification mechanism based on seawater vacuolization, if there was not the need to fractionate strongly against Mg. Active removal of Mg by Mg^{2+} transporters has been suggested to account for the Mg fractionation (Erez, 2003). For this idea to be compatible with our data, the Mg transporter would have to remove Mg, in proportion to the seawater Mg / Ca, independent of the seawater Mg concentration. A physiological basis for such a scenario is hard to envision. Therefore we conclude that our data argue against the vacuolization model.

Foraminiferal Mg/Ca_{CC} at varying Mg/Ca_{sw} can be used to test the biomineralization model developed by Nehrke et al. (2013). This model assumes that foraminifers obtain the majority of Ca^{2+} , needed for calcification, via highly selective transmembrane transport (TMT) and that the majority of the Mg^{2+} stems from (unfractionated) seawater leakage or vacuolar transport (i.e. “passive transport” (PT)). In contrast to the vacuole-based biomineralization model (e.g. Bentov and Erez, 2006; Bentov et al., 2009), the

Impact of seawater Ca^{2+} on the calcification

A. Mewes et al.

Title Page

Abstract

Introduction

Conclusions

References

Tables

Figures



Back

Close

Full Screen / Esc

Printer-friendly Version

Interactive Discussion



TMT/PT mixing model assumes that the percentage of ions transported via PT, is very small compared to those delivered by TMT. Given that elements are not fractionated during the transport of vacuoles to the site of calcification, contribution from vacuole-bound ions or seawater leakage plays a key role in determining the Mg/Ca_{CC} . The model explains the difference between low, medium and high-Mg calcite species via an increasing relative contribution of PT. As already suggested by Nehrke et al. (2013), the model predictions can be tested with culture studies such as this one.

As discussed by Mewes et al. (2014), the relationship between Mg/Ca_{CC} and Mg/Ca_{SW} is best described by a linear relationship having a positive intercept (Fig. 6a). At high Mg/Ca_{SW} this relationship is in line with the mixing model (Nehrke et al., 2013). At very low Mg/Ca_{SW} , however, the present and our previous data have a positive y intercept, i.e. an increased D_{Mg} (Fig. 6b), which is not predicted by the model of Nehrke et al. (2013) (for discussion see Mewes et al., 2014). Here we present a refined flux-based model, which solves this problem (for the mathematical derivation see Appendix). The model is based on the same assumptions as Nehrke et al. (2013): the total ion flux is divided into passive transport (PT) and transmembrane transport (TMT) (mixing model). The fraction of the total flux of the divalent cations transported via PT, is expressed as x (see Eq. A2). Similar to Nehrke et al. (2013), we assume no fractionation during passive transport, while we assume a strong fractionation (frac) during TMT (see Eqs. A4 and A5). The Mg/Ca_{CC} ratio of the precipitated calcite represents the Mg/Ca ratio of the two different fluxes (see Eq. A10). A further fundamental assumption is that Mg^{2+} substitutes for Ca^{2+} in the calcite lattice, i.e. in a given volume of calcite the sum of Mg and Ca ions is constant. Based on data showing high Mg areas in conjunction with organic layers in the shell, it was traditionally assumed that Mg^{2+} may be incorporated in the organic layers, rather than in the calcite lattice alone (Erez, 2003). However, by means of nano-scale synchrotron X-ray spectroscopy, Branston et al. (2013) showed that most of the Mg present in foraminiferal shells substitutes for Ca in the calcite lattice. Therefore the assumption that the sum of Mg and Ca is constant is justified.

Impact of seawater Ca^{2+} on the calcification

A. Mewes et al.

[Title Page](#)[Abstract](#)[Introduction](#)[Conclusions](#)[References](#)[Tables](#)[Figures](#)[Back](#)[Close](#)[Full Screen / Esc](#)[Printer-friendly Version](#)[Interactive Discussion](#)

Based on the above assumptions the refined flux-based model yields calcite Mg / Ca

$$\left(\frac{\text{Mg}^{2+}}{\text{Ca}^{2+}}\right)_{\text{CC}} = R_{\text{SW}} \left[\frac{\text{frac}(1-x) + x + \text{frac} \cdot R_{\text{SW}}}{1 + (1-x + \text{frac} \cdot x)R_{\text{SW}}} \right] \quad (3)$$

The curve (Fig. 7a) can be fitted over the whole Mg/Ca_{SW} with a TMT fractionation frac = 0.005 and a contribution of PT to the total ion flux x = 0.02. The TMT fractionation, i.e. 0.005 (= frac) is weaker than the one assumed in the previous model (0.0001; Nehrke et al., 2013). This is a reasonable modification because Mg TMT fractionation is not known in either coccolithophores or foraminifera and typical Ca channels display a range of Mg fractionation (e.g. White, 2000).

The partition coefficient for Mg is given by:

$$D_{\text{Mg}^{2+}} = \left(\frac{\text{Mg}^{2+}}{\text{Ca}^{2+}}\right)_{\text{CC}} / R_{\text{SW}} = \frac{\text{frac}(1-x) + x + \text{frac} \cdot R_{\text{SW}}}{1 + (1-x + \text{frac} \cdot x)R_{\text{SW}}} \quad (4)$$

This refined flux-based model predicts both the trend of Mg/Ca_{CC} vs. Mg/Ca_{SW} and D_{Mg} vs. Mg/Ca_{SW}. Especially the dependence of D_{Mg} on Mg/Ca_{SW} is interesting because the trend observed here (Figs. 6b and 7b) was also reported for inorganically precipitated calcite (Mucci and Morse, 1983). Segev and Erez (2006) already noted that curious fact. They commented: “A physiological mechanism sensitive to ratio . . . remains to be explored” (Segev and Erez, 2006). We present such a physiological mechanism. Our refined flux-based model for major and minor element incorporation therefore represents a promising new way of interpreting foraminiferal element to calcium ratios. Future research should hence be concerned with the question whether the behavior of other elements can be reconciled with our model.

Impact of seawater Ca²⁺ on the calcification

A. Mewes et al.

Title Page

Abstract

Introduction

Conclusions

References

Tables

Figures



Back

Close

Full Screen / Esc

Printer-friendly Version

Interactive Discussion



5 Summary

Our study showed optimum growth performance of *Amphistegina lessonii* at Mg/Ca_{SW} near ambient. Growth rates, test wall thickness and also test Mg/Ca_{CC} is not controlled by absolute seawater [Ca] and [Mg], but by their ratio in seawater. We provide further support for the recently developed biomineralization model by Nehrke et al. (2013) and present a refined flux-based model which predicts our experimentally determined dependence of Mg/Ca_{CC} on Mg/Ca_{SW}.

Appendix A: Refined TMT+PT mixing model

The transport of Mg²⁺ and Ca²⁺ in our flux-based model is described in terms of the total flux of the bivalent cations

$$F_{CAT} = F_{Ca^{2+}} + F_{Mg^{2+}}. \quad (A1)$$

The total ion flux is sub-divided into passive transport (PT) and transmembrane transport (TMT). Assuming that a fraction x of the total flux is transported via PT, the fluxes of bivalent cations for both transport pathways are expressed as

$$F_{PT} = F_{PT,Ca^{2+}} + F_{PT,Mg^{2+}} = xF_{CAT} \quad (A2)$$

$$F_{TMT} = F_{TMT,Ca^{2+}} + F_{TMT,Mg^{2+}} = (1 - x)F_{CAT} \quad (A3)$$

The contribution of Ca²⁺ and Mg²⁺ to PT and TMP is controlled by the fractionation during transport. It is assumed that no fractionation takes place during passive transport, but a strong fractionation (frac) during TMT. Based on this assumption the ratios

BGD

11, 17463–17489, 2014

Impact of seawater Ca²⁺ on the calcification

A. Mewes et al.

Title Page

Abstract

Introduction

Conclusions

References

Tables

Figures

◀

▶

◀

▶

Back

Close

Full Screen / Esc

Printer-friendly Version

Interactive Discussion



of Ca^{2+} and Mg^{2+} fluxes are given by

$$\frac{F_{\text{PT},\text{Mg}^{2+}}}{F_{\text{PT},\text{Ca}^{2+}}} = R_{\text{SW}}, \quad (\text{A4})$$

$$\frac{F_{\text{TMT},\text{Mg}^{2+}}}{F_{\text{TMT},\text{Ca}^{2+}}} = \text{frac} \cdot R_{\text{SW}}, \quad (\text{A5})$$

where R_{SW} is the seawater Mg / Ca. Combination of Eqs. (A2)–(A5) yields the Ca^{2+} and Mg^{2+} fluxes for the PT and TMT pathways

$$F_{\text{PT},\text{Mg}^{2+}} = \frac{R_{\text{SW}}}{1 + R_{\text{SW}}} x \cdot F_{\text{CAT}}, \quad (\text{A6})$$

$$F_{\text{PT},\text{Ca}^{2+}} = \frac{1}{1 + R_{\text{SW}}} x \cdot F_{\text{CAT}}, \quad (\text{A7})$$

$$F_{\text{TMT},\text{Mg}^{2+}} = \frac{\text{frac} \cdot R_{\text{SW}}}{1 + \text{frac} \cdot R_{\text{SW}}} (1 - x) F_{\text{CAT}}, \quad (\text{A8})$$

$$F_{\text{TMT},\text{Ca}^{2+}} = \frac{1}{1 + \text{frac} \cdot R_{\text{SW}}} (1 - x) F_{\text{CAT}}. \quad (\text{A9})$$

The Mg/Ca_{CC} ratio of the precipitated calcite represents the Mg / Ca ratio of the ion fluxes:

$$\left(\frac{\text{Mg}^{2+}}{\text{Ca}^{2+}} \right)_{\text{CC}} = \frac{F_{\text{TMT},\text{Mg}^{2+}} + F_{\text{PT},\text{Mg}^{2+}}}{F_{\text{TMT},\text{Ca}^{2+}} + F_{\text{PT},\text{Ca}^{2+}}} = \frac{\frac{\text{frac} \cdot R_{\text{SW}}}{1 + \text{frac} \cdot R_{\text{SW}}} (1 - x) F_{\text{CAT}} + \frac{R_{\text{SW}}}{1 + R_{\text{SW}}} x \cdot F_{\text{CAT}}}{\frac{1}{1 + \text{frac} \cdot R_{\text{SW}}} (1 - x) F_{\text{CAT}} + \frac{1}{1 + R_{\text{SW}}} x \cdot F_{\text{CAT}}}, \quad (\text{A10})$$

which can be written as:

$$\left(\frac{\text{Mg}^{2+}}{\text{Ca}^{2+}} \right)_{\text{CC}} = R_{\text{SW}} \left[\frac{\text{frac} (1 - x) + x + \text{frac} \cdot R_{\text{SW}}}{1 + (1 - x + \text{frac} \cdot x) R_{\text{SW}}} \right]. \quad (\text{A11})$$

17477

Impact of seawater Ca^{2+} on the calcification

A. Mewes et al.

Title Page

Abstract

Introduction

Conclusions

References

Tables

Figures



Back

Close

Full Screen / Esc

Printer-friendly Version

Interactive Discussion



Impact of seawater Ca^{2+} on the calcification

A. Mewes et al.

Title Page

Abstract

Introduction

Conclusions

References

Tables

Figures



Back

Close

Full Screen / Esc

Printer-friendly Version

Interactive Discussion



Equation (A11) indicates that the calcite Mg / Ca depends on the seawater Mg / Ca , but not on the total flux of the bivalent cations (F_{CAT}). This explains why test Mg / Ca is controlled by the ratio of Mg and Ca , but not by their absolute concentrations in seawater. The partition coefficient for Mg ($D_{\text{Mg}^{2+}}$) is defined with respect to seawater

Mg / Ca , thus

$$D_{\text{Mg}^{2+}} = \left(\frac{\text{Mg}^{2+}}{\text{Ca}^{2+}} \right)_{\text{CC}} / R_{\text{SW}} = \frac{\text{frac}(1-x) + x + \text{frac} \cdot R_{\text{SW}}}{1 + (1-x + \text{frac} \cdot x) R_{\text{SW}}} \quad (\text{A12})$$

Acknowledgements. Max Janse and his team are acknowledged for providing specimens from a coral reef tank at Burger's Zoo, in Arnhem, the Netherlands. Laura Wischnewski is acknowledged for her assistance with culturing foraminifers. We furthermore like to thank the technical assistance of Ulrike Richter, who prepared algae cultures, Jana Hölscher for doing DIC measurements, Ilsetraut Stöltling for doing ICP-OES analyses and Helen de Waard for assisting during LA-ICP-MS analyzes at Utrecht University. This work was funded in part by The European Research Council (ERC grant 2010-NEWLOG ADG-267931 HE).

References

- Branson, O., Redfern, S. A., Tyliszczak, T., Sadekov, A., Langer, G., Kimoto, K., and Elderfield, H.: The coordination of Mg in foraminiferal calcite, *Earth Planet. Sc. Lett.*, 383, 134–141, 2013.
- Broecker, W. and Yu, J.: What do we know about the evolution of Mg to Ca ratios in seawater?, *Paleoceanography*, 26, PA3203, doi:10.1029/2011PA002120, 2006.
- Bentov, S. and Erez, J.: Impact of biomineralization processes on the Mg content of foraminiferal shells: a biological perspective, *Geochem. Geophys. Geosy.*, 7, 1–11, 2006.
- Bentov, S., Brownlee, C., and Erez, J.: The role of seawater endocytosis in the biomineralization process in calcareous foraminifera, *P. Natl. Acad. Sci. USA*, 106, 21500–21504, 2009.
- de Nooijer, L. J., Langer, G., Nehrke, G., and Bijma, J.: Physiological controls on seawater uptake and calcification in the benthic foraminifer *Ammonia tepida*, *Biogeosciences*, 6, 2669–2675, doi:10.5194/bg-6-2669-2009, 2009.

Impact of seawater Ca^{2+} on the calcification

A. Mewes et al.

Title Page

Abstract

Introduction

Conclusions

References

Tables

Figures



Back

Close

Full Screen / Esc

Printer-friendly Version

Interactive Discussion



- de Nooijer, L. J., Spero, H. J., Erez, J., Bijma, J., and Reichart, G. J.: Biomineralization in perforate foraminifera, *Earth-Science Reviews*, 135, 48–58, 2014.
- Dueñas-Bohórquez, A., Da Rocha, R. E., Kuroyanagi, A., Bijma, J., and Reichart, G. J.: Effect of salinity and seawater calcite saturation state on Mg and Sr incorporation in cultured planktonic foraminifera, *Mar. Micropaleontol.*, 73, 178–189, 2009.
- Dueñas-Bohórquez, A., Da Rocha, R. E., Kuroyanagi, A., De Nooijer, L. J., Bijma, J., and Reichart, G. J.: Interindividual variability and ontogenetic effects on Mg and Sr incorporation in the planktonic foraminifer *Globigerinoides sacculifer*, *Geochim. Cosmochim. Ac.*, 75, 520–532, 2011.
- Erez, J.: The source of ions for biomineralization in foraminifera and their implications for paleoceanographic proxies, *Rev. Mineral. Geochem.*, 54, 115–149, 2003.
- Ernst, S., Janse, M., Renema, W., Kouwenhoven, T., Goudeau, M. L., and Reichart, G. J.: Benthic foraminifera in a large Indo-Pacific coral reef aquarium, *J. Foramin. Res.*, 41, 101–113, 2011.
- Evans, D. and Müller, W.: Deep time foraminifera Mg / Ca paleothermometry: nonlinear correction for secular change in seawater Mg / Ca, *Paleoceanography*, 27, 1–11, 2012.
- Glas, M. S., Langer, G., and Keul, N.: Calcification acidifies the microenvironment of a benthic foraminifer (*Ammonia sp.*), *J. Exp. Mar. Biol. Ecol.*, 424, 53–58, 2012.
- Hardie, L. A.: Secular variation in seawater chemistry: an explanation for the coupled secular variation in the mineralogies of marine limestones and potash evaporites over the past 600 my, *Geology*, 24, 279–283, 1996.
- Hoppe, C. J. M., Langer, G., and Rost, B.: *Emiliania huxleyi* shows identical responses to elevated $p\text{CO}_2$ in TA and DIC manipulations, *J. Exp. Mar. Biol. Ecol.*, 406, 54–62, 2011.
- Jochum, K. P., Weis, U., Stoll, B., Kuzmin, D., Yang, Q. C., Raczek, I., Jacob, D. E., Stracke, A., Birbaum, K., Frick, D. A., Gunther, D., and Enzweiler, J.: Determination of reference values for NIST SRM 610-617 glasses following ISO guidelines, *Geostand. Geoanal. Res.*, 35, 397–429, 2011.
- Kester, D. R., Duedall, I. W., Connors, D. N., and Pytkowicz, R. M.: Preparation of artificial seawater, *Limnol. Oceanogr.*, 12, 176–179, 1967.
- Keul, N., Langer, G., de Nooijer, L. J., and Bijma, J.: Effect of ocean acidification on the benthic foraminifera *Ammonia sp.* is caused by a decrease in carbonate ion concentration, *Biogeosciences*, 10, 6185–6198, doi:10.5194/bg-10-6185-2013, 2013.

Impact of seawater Ca^{2+} on the calcification

A. Mewes et al.

Title Page

Abstract

Introduction

Conclusions

References

Tables

Figures



Back

Close

Full Screen / Esc

Printer-friendly Version

Interactive Discussion



- Lear, C. H., Elderfield, H., and Wilson, P. A.: Cenozoic deep-sea temperatures and global ice volumes from Mg / Ca in benthic foraminiferal calcite, *Science*, 287, 269–272, 2000.
- Lee, A. and East, J.: What the structure of a calcium pump tells us about its mechanism, *Biochem. J.*, 356, 665–683, 2001.
- 5 Martínez-Colón, M., Hallock, P., and Green-Ruíz, C.: Strategies for using shallow-water benthic foraminifers as bioindicators of potentially toxic elements: a review, *J. Foramin. Res.*, 39, 278–299, 2009.
- Mewes, A., Langer, G., de Nooijer, L. J., Bijma, J., and Reichart, J. G.: Effect of different seawater Mg^{2+} concentrations on calcification in two benthic foraminifers, *Mar. Micropaleontol.*, 10
113, 56–64, 2014.
- Mucci, A. and Morse, J. W.: The incorporation of Mg^{2+} and Sr^{2+} into calcite overgrowths: influences of growth rate and solution composition, *Geochim. Cosmochim. Ac.*, 47, 217–233, 1983.
- Nehrke, G., Keul, N., Langer, G., de Nooijer, L. J., Bijma, J., and Meibom, A.: A new model for biomineralization and trace-element signatures of Foraminifera tests, *Biogeosciences*, 10, 6759–6767, doi:10.5194/bg-10-6759-2013, 2013.
- 15 Nelson, D. L. and Cox, M. M.: *Lehninger Principles of Biochemistry*, W. H. Freeman, 6th revised international edn., 2013.
- Nürnberg, D., Bijma, J., and Hemleben, C.: Assessing the reliability of magnesium in foraminiferal calcite as a proxy for water mass temperatures, *Geochim. Cosmochim. Ac.*, 20
60, 803–814, 1996.
- Raitzsch, M., Dueñas-Bohórquez, A., Reichart, G.-J., de Nooijer, L. J., and Bickert, T.: Incorporation of Mg and Sr in calcite of cultured benthic foraminifera: impact of calcium concentration and associated calcite saturation state, *Biogeosciences*, 7, 869–881, doi:10.5194/bg-7-869-2010, 2010.
- 25 Segev, E. and Erez, J.: Effect of Mg / Ca ratio in seawater on shell composition in shallow benthic foraminifera, *Geochem. Geophys. Geosy.*, 7, 1–8, 2006.
- Spero, H. J.: Ultrastructural examination of chamber morphogenesis and biomineralization in the planktonic foraminifer *Orbulina universa*, *Mar. Biol.*, 99, 9–20, 1988.
- 30 Signes, M., Bijma, J., Hemleben, C., and Ott, R.: A model for planktic foraminiferal shell growth, *Paleobiology*, 19, 71–91, 1993.
- Ter Kuile, B., Erez, J., and Padan, E.: Mechanisms for the uptake of inorganic carbon by two species of symbiont-bearing foraminifera, *Mar. Biol.*, 103, 241–251, 1989.

BGD

11, 17463–17489, 2014

Impact of seawater Ca^{2+} on the calcification

A. Mewes et al.

Title Page

Abstract

Introduction

Conclusions

References

Tables

Figures



Back

Close

Full Screen / Esc

Printer-friendly Version

Interactive Discussion



Impact of seawater Ca^{2+} on the calcification

A. Mewes et al.

Table 1. Details of culture media.

	<i>Amphistegina lessonii</i>					
	treat. 1	treat. 2	treat. 3	treat. 4	treat. 5	treat. 6
SW Mg^{2+} [mM]	51.64	52.56	52.75	52.66	52.05	52.40
SW Ca^{2+} [mM]	34.19	17.86	9.22	6.63	4.77	3.18
Mg/ Ca_{SW} [mol mol^{-1}]	1.51	2.94	5.72	7.95	10.91	16.47
± st. error	± 0.00	± 0.03	± 0.02	± 0.05	± 0.07	± 0.09
Mg/ Ca_{CC} [mmol mol^{-1}]	22.95	40.79	52.08	67.50	83.35	–
± st. error	± 0.81	± 1.38	± 1.72	± 2.37	± 1.96	
T [$^{\circ}\text{C}$]	25	25	25	25	25	25
S [%]	32.4	32.4	32.4	32.4	32.4	32.4
pH (NBS)	8.1	8.1	8.1	8.1	8.1	8.1
TA [$\mu\text{mol kg}^{-1}$]	2615	2545	2504	2504	2492	2479
Ω (calcite)	16.75	8.74	4.49	3.24	2.33	1.55
DIC [$\mu\text{mol kg}^{-1}$]	2302	2298	2286	2295	2294	2290

Title Page

Abstract

Introduction

Conclusions

References

Tables

Figures



Back

Close

Full Screen / Esc

Printer-friendly Version

Interactive Discussion



Impact of seawater Ca^{2+} on the calcification

A. Mewes et al.

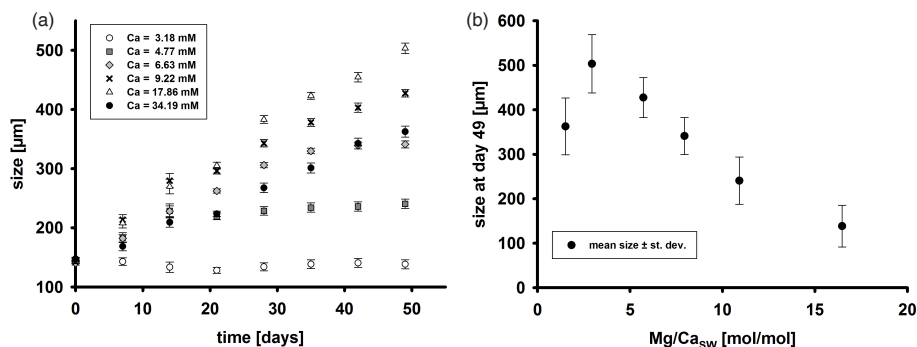


Figure 1. (a) Mean test size \pm st. error for all treatments vs. time in culture ($n = 37$ – 56). (b) Mean test size \pm SD at the end of the experiment vs. seawater Mg / Ca.

Title Page

Abstract

Introduction

Conclusions

References

Tables

Figures



Back

Close

Full Screen / Esc

Printer-friendly Version

Interactive Discussion



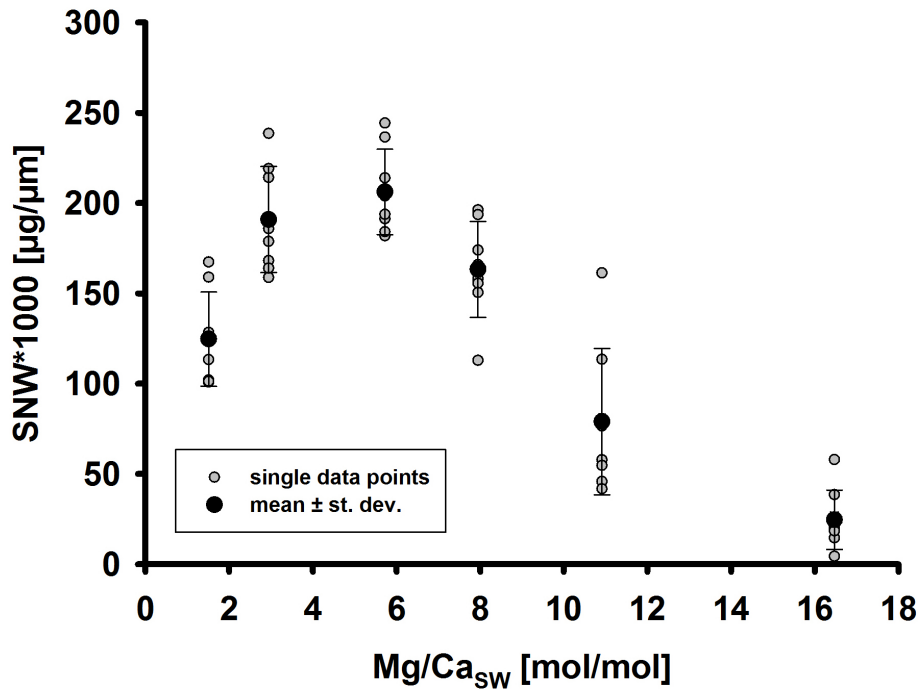


Figure 2. Size normalized weight vs. seawater Mg / Ca ($n = 8$).

Impact of seawater Ca^{2+} on the calcification

A. Mewes et al.

Title Page

Abstract

Introduction

Conclusions

References

Tables

Figures



Back

Close

Full Screen / Esc

Printer-friendly Version

Interactive Discussion



Impact of seawater Ca^{2+} on the calcification

A. Mewes et al.

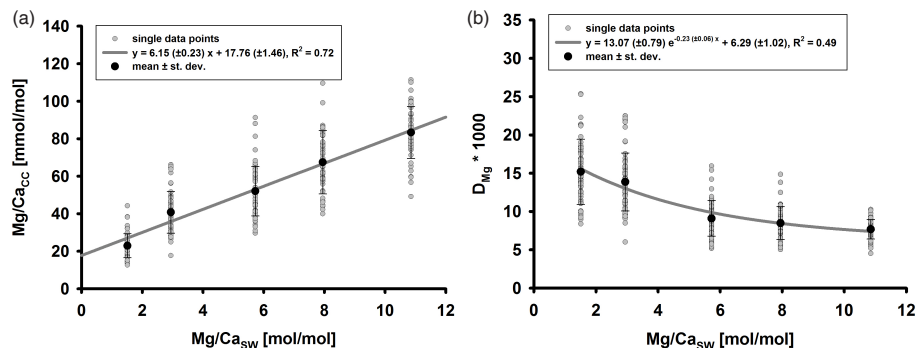


Figure 3. (a) $\text{Mg}/\text{Ca}_{\text{CC}}$ vs. $\text{Mg}/\text{Ca}_{\text{SW}}$ ([Ca] and thus Ω decreases with increasing $\text{Mg}/\text{Ca}_{\text{SW}}$) and (b) $D_{\text{Mg}} \times 1000$ vs. $\text{Mg}/\text{Ca}_{\text{SW}}$ ($n = 50$ – 65 ablations per treatment).

Title Page

Abstract

Introduction

Conclusions

References

Tables

Figures



Back

Close

Full Screen / Esc

Printer-friendly Version

Interactive Discussion



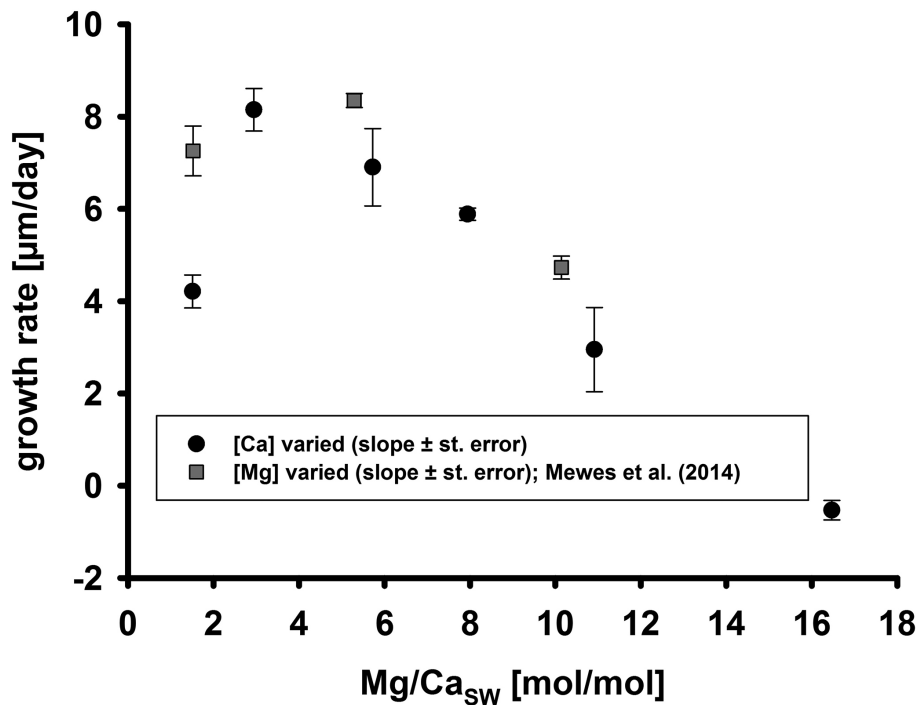


Figure 4. Growth rates [$\mu\text{m day}^{-1}$], derived from linear regression curves fitted to size data of the first 30 days in culture, vs. $\text{Mg}/\text{Ca}_{\text{SW}}$.

Impact of seawater Ca^{2+} on the calcification

A. Mewes et al.

Title Page

Abstract Introduction

Conclusions References

Tables Figures

◀ ▶

◀ ▶

Back Close

Full Screen / Esc

Printer-friendly Version

Interactive Discussion



Impact of seawater Ca^{2+} on the calcification

A. Mewes et al.

Title Page

Abstract

Introduction

Conclusions

References

Tables

Figures

◀

▶

◀

▶

Back

Close

Full Screen / Esc

Printer-friendly Version

Interactive Discussion

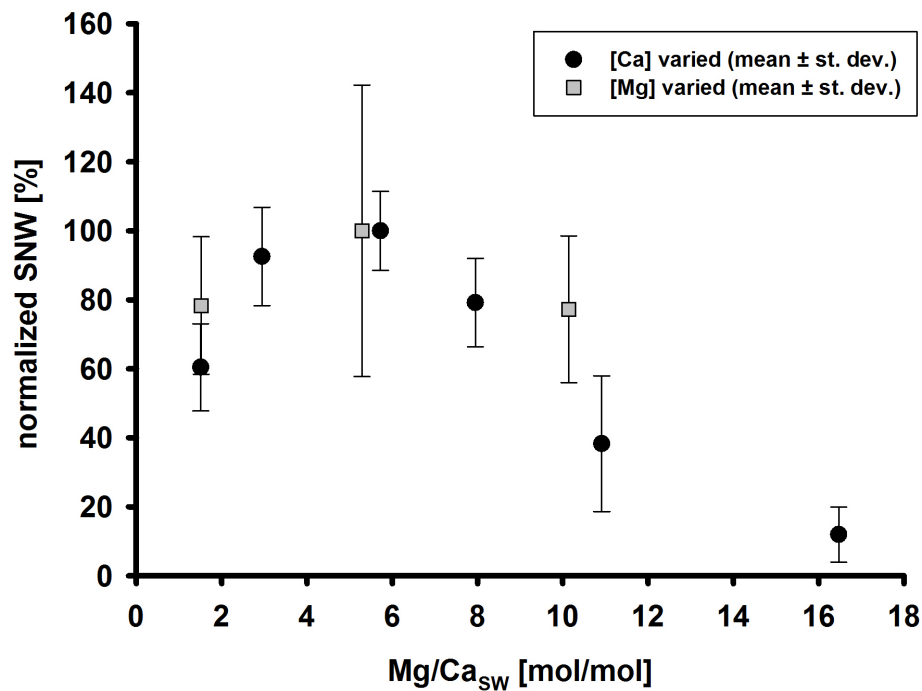


Figure 5. % mean size normalized weight [$\mu\text{g}\mu\text{m}^{-1}$] vs. $\text{Mg}/\text{Ca}_{\text{SW}}$.

Impact of seawater Ca^{2+} on the calcification

A. Mewes et al.

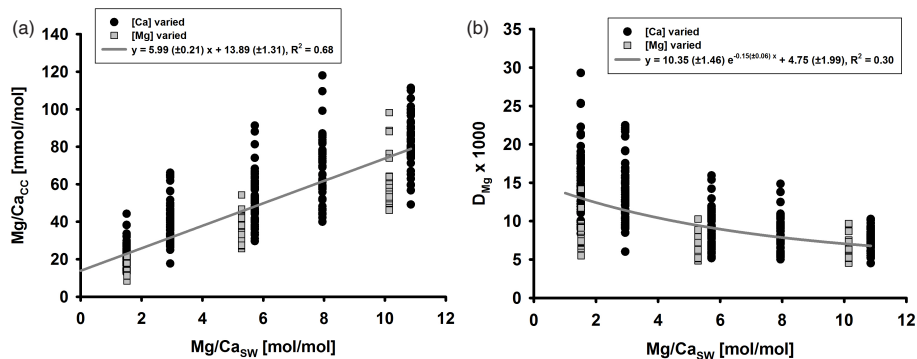


Figure 6. (a) $\text{Mg}/\text{Ca}_{\text{CC}}$ vs. $\text{Mg}/\text{Ca}_{\text{SW}}$. (b) $D_{\text{Mg}} \times 1000$ vs. $\text{Mg}/\text{Ca}_{\text{SW}}$.

Title Page

Abstract

Introduction

Conclusions

References

Tables

Figures



Back

Close

Full Screen / Esc

Printer-friendly Version

Interactive Discussion



Impact of seawater Ca^{2+} on the calcification

A. Mewes et al.

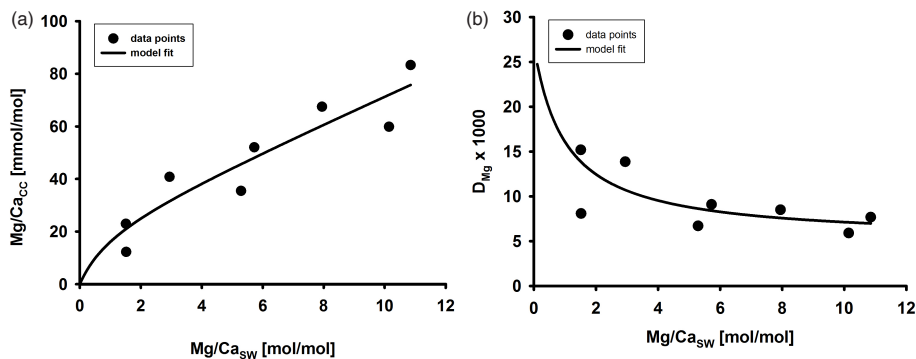


Figure 7. Model fit to the data of our present and previous study (Mewes et al., 2014) for **(a)** $\text{Mg}/\text{Ca}_{\text{CC}}$ vs. $\text{Mg}/\text{Ca}_{\text{SW}}$. **(b)** $D_{\text{Mg}} \times 1000$ vs. $\text{Mg}/\text{Ca}_{\text{SW}}$.

[Title Page](#)[Abstract](#)[Introduction](#)[Conclusions](#)[References](#)[Tables](#)[Figures](#)[⏪](#)[⏩](#)[◀](#)[▶](#)[Back](#)[Close](#)[Full Screen / Esc](#)[Printer-friendly Version](#)[Interactive Discussion](#)